HHS Public Access

Author manuscript

J Magn Reson Imaging. Author manuscript; available in PMC 2021 February 01.

Published in final edited form as:

J Magn Reson Imaging. 2019 June ; 49(7): e183–e194. doi:10.1002/jmri.26582.

Combined 5-Minute Double-Echo in Steady-State With Separated Echoes and 2-Minute Proton-Density-Weighted 2D FSE Sequence for Comprehensive Whole-Joint Knee MRI Assessment

Akshay S. Chaudhari, PhD[1,2,*], **Kathryn J. Stevens, MD**[1,3], **Bragi Sveinsson, PhD**[1,4,5], **Jeff P. Wood, MD**[1], **Christopher F. Beaulieu, MD, PhD**[1,3], **Edwin H.G. Oei, MD, PhD**[6], **Jarrett K. Rosenberg, PhD**[1], **Feliks Kogan, PhD**[1], **Marcus T. Alley, PhD**[1], **Garry E. Gold, MD**[1,2,3], **Brian A. Hargreaves, PhD**[1,2,7]

[1]Department of Radiology, Stanford University, Stanford, California, USA; [2]Department of Bioengineering, Stanford University, Stanford, California, USA; [3]Department of Orthopaedic Surgery, Stanford University, Stanford, California, USA; [4]Athinoula A. Martinos Center for Biomedical Imaging, Massachusetts General Hospital, Boston, Massachusetts, USA; [5]Department of Radiology, Harvard Medical School, Boston, Massachusetts, USA; [6]Department of Radiology & Nuclear Medicine, Erasmus MC, University Medical Center, Rotterdam, The Netherlands; [7]Department of Electrical Engineering, Stanford University, Stanford, California, USA

Abstract

Background: Clinical knee MRI protocols require upwards of 15 minutes of scan time.

Purpose/Hypothesis: To compare the imaging appearance of knee abnormalities depicted with a 5-minute 3D double-echo in steady-state (DESS) sequence with separate echo images, with that of a routine clinical knee MRI protocol. A secondary goal was to compare the imaging appearance of knee abnormalities depicted with 5-minute DESS paired with a 2-minute coronal proton-density fat-saturated (PDFS) sequence.

Study Type: Prospective.

Subjects: Thirty-six consecutive patients (19 male) referred for a routine knee MRI.

Field Strength/Sequences: DESS and PDFS at 3T.

Assessment: Five musculoskeletal radiologists evaluated all images for the presence of internal knee derangement using DESS, DESS+PDFS, and the conventional imaging protocol, and their associated diagnostic confidence of the reading.

[*]Address reprint requests to: A.C., Department of Radiology, Stanford University, Lucas Center for Imaging, 1201 Welch Road P064-n, Stanford, CA, 94305. akshaysc@stanford.edu.

Disclosure

A.C. has provided consulting services to Skope MR Inc and Subtle Medical. Neither organizations were involved in the design, execution, data analysis, or the reporting of this study.

Statistical Tests: Differences in positive and negative percent agreement (PPA and NPA, respectively) and 95% confidence intervals (CIs) for DESS and DESS+PDFS compared with the conventional protocol were calculated and tested using exact McNemar tests. The percentage of observations where DESS or DESS+PDFS had equivalent confidence ratings to DESS+Conv were tested with exact symmetry tests. Interreader agreement was calculated using Krippendorff's alpha.

Results: DESS had a PPA of 90% (88–92% CI) and NPA of 99% (99–99% CI). DESS+PDFS had increased PPA of 99% (95–99% CI) and NPA of 100% (99–100% CI) compared with DESS (both $P < 0.001$). DESS had equivalent diagnostic confidence to DESS+Conv in 94% of findings, whereas DESS+PDFS had equivalent diagnostic confidence in 99% of findings (both $P < 0.001$). All readers had moderate concordance for all three protocols (Krippendorff's alpha 47–48%).

Data Conclusion: Both 1) 5-minute 3D-DESS with separated echoes and 2) 5-minute 3D-DESS paired with a 2-minute coronal PDFS sequence depicted knee abnormalities similarly to a routine clinical knee MRI protocol, which may be a promising technique for abbreviated knee MRI.

There are approximately 1.25 million clinical knee magnetic resonance imaging (MRI) scans performed annually in the US.[1,2] Most extremity and knee MRI protocols consist mainly of 2D fast-spin-echo (FSE) sequences with different combinations of contrasts, fat-suppression, and orientations, requiring ~20 minutes of scan time. 2D FSE sequences typically employ a high in-plane resolution (0.3–0.6 mm) but acquire thicker slices (>2.5 mm) with gaps between adjacent slices due to limitations of scan time. Apart from modest parallel imaging accelerations, the use of additional acceleration methods such as compressed sensing and simultaneous multislice (SMS) do not have widespread clinical adoption. Consequently, there is interest in faster sequences that provide high in-plane and through-plane resolution in order to overcome partial volume effects and to allow visualization of tissues in arbitrary scan planes, especially with the push towards "high-value" imaging.[3]

Advancements in parallel imaging and SMS research have shown promising results to accelerate 2D FSE protocols for knee MRI; however, such methods still preclude oblique slice reformations due to the acquisition of slices with high section-thickness.[4,5] 3D-FSE sequences are promising for fast imaging[6–8]; however, the diagnostic potential of such sequences may be limited due to image blurring induced by long echo trains. 3D balanced steady-state free-precession (bSSFP) sequences have also been explored, but bSSFP produces only singular contrast, which may not be adequate for comprehensive musculoskeletal imaging, and fat suppression is not always robust.[9,10] The water-selective 3D double-echo in steady-state (DESS) sequence with separated echoes, on the other hand, may overcome such limitations, as it produces dual-contrasts without echo-train blurring along with quantitative T_2 relaxation time maps.

DESS samples two 3D echoes where the first echo (S+) has a T_1/T_2 weighting (similar to a proton-density [PD] weighting in the knee), while the second echo (S−) has an additional T_2 weighting.[11–13] While many available DESS methods (most commonly the Siemens product that is used in the Osteoarthritis Initiative) combine these echoes into a single image; the DESS sequence in this work reconstructs two individual echo images separately as

originally proposed.[11–13] DESS S + has a gradient-spoiled contrast (fast imaging with steady-state precession (FISP), fast-field echo (FFE), gradient recall echo (GRE), gradient recalled acquisition in steady state (GRASS), or Fourier acquired steady state (FAST) on different scanners), high signal-to-noise ratio (SNR), and reduced sensitivity to motion. DESS S− has a longer echo time and consequently an additional T_2-weighting, similar to PSIF, T_2-FFE, and CE-FAST methods, which provides higher fluid sensitivity.

DESS with separated echo images has engendered high accuracy for semiquantitative whole-knee-joint assessment using the MRI Osteoarthritis Knee Score (MOAKS).[14,15] The two DESS echoes can also be used to generate accurate and automatic T_2 measurements of the articular cartilage and the meniscus using analytical expressions.[16,17] The T_2 relaxation time has primarily been studied in the context of early osteoarthritis progression in collagenous tissues.[18,19] However, the role of T_2 mapping has been relatively unexplored diagnostically, likely due to the challenges in acquiring T_2 efficiently in clinically feasible scan durations.

Given the previous benefits of DESS, the purpose of this exploratory study was to compare the imaging appearance of knee abnormalities depicted with a single 5-minute 3D-DESS sequence with separate echo images, to that of a routine clinical knee MRI protocol for assessing bone, cartilage, ligaments, menisci, tendons, and synovium. Additionally, for studying the utility of abbreviated knee MRI protocols, the secondary goal of this study was to compare the imaging appearance of knee abnormalities depicted with a 5-minute DESS scan paired with a 2-minute coronal proton-density fat-saturated (PDFS) scan. Comparisons to arthroscopic surgery were performed for patients who underwent surgery.

Materials and Methods

Patient Recruitment and MRI Protocol

Thirty-six consecutive patients (19 male, age 45 ± 18 years, and 17 female age 41 ± 20 years) between October 2016 and November 2016 were scanned with Institutional Review Board approval, informed consent, and Health Insurance Portability and Accountability Act compliance for this prospective study. The inclusion criteria included patients referred for a routine knee MRI by physicians while the exclusion criteria included contraindications to MRI or excessive motion artifacts in images. All scans were performed on one of two identical Discovery MR750 3.0T MRI scanners (GE Healthcare, Waukesha, WI) with an 8-channel transmit-receive knee coil (InVivo, Gainesville, FL).

A water-excitation sagittal 3D-DESS sequence was added to the end of the routine knee protocol that consisted of a total of five sequences with PD-weighting, T_1-weighting, and T_2-weighting (scan parameters in Table 1). A 20° flip angle was chosen for DESS in order to maximize the tissue SNR for morphological imaging as well as accurate T_2 measurements for cartilage and meniscus.[14] A 3.4 msec spatial-spectral RF pulse consisting of six spatially selective sub-lobes was used for selective water-only excitation while maintaining a low repetition time. The sagittal DESS sequence was used to perform multiplanar reformatting (MPR) of both echo images. Autocalibrating parallel imaging (acPI) reconstruction was used to accelerate the DESS scan by a factor of 2 in the phase-encode direction (2 × 1 acPI).

acPI does not require a calibration scan and is thereby less affected by motion between the calibration and target scans. Additionally, acPI is more robust than sensitivity encoding (SENSE) when the coil sensitivity map is changing rapidly due to the existence of fine tissue structures, as is common in knee imaging.[20] Image reconstruction for DESS was performed automatically on the scanner computer. The duration of the conventional protocol, excluding the localizer/scout scan but including prescanning, a coil sensitivity calibration scan for parallel imaging, and any repeated scans was recorded.

T_2 relaxation times maps were generated automatically on the scanner computer as an additional imaging series using an analytical expression involving a ratio of the two DESS echoes, as described previously.[14,21] MPR of both DESS echoes and T_2 maps were submitted immediately to the picture archiving and communication system (PACS). While the T_2 relaxation time maps were not explicitly used in the reader study, the T_2 maps were retrospectively visualized for commonly indicated abnormalities. The goal for such an exercise was to understand the appearance of common abnormalities on T_2 maps to assess whether the addition of T_2 maps could be useful in future routine clinical knee MRI examinations.

Image Analysis

Four board-certified musculoskeletal radiologists (K.S., C.B., E.O., and G.G., with 18, 22, 13, and 18 years of experience, respectively) and one musculoskeletal fellow (J.W. with 1 year of experience), evaluated all images for the presence of 30 common imaging findings in internal derangements of the knee, subdivided into categories of bone, cartilage, ligaments, menisci, synovium, and tendons (Table 2). All patient scans were independently reviewed in a randomized order between the five readers. The readers recorded the presence of all 30 imaging findings (Yes/No) and scored the diagnostic confidence of the sequences used (0 = No Confidence, 1 = Low Confidence, 2 = Moderate Confidence, and 3 = High Confidence). Since collateral ligaments and tendons can have a wide spectrum of imaging appearances, MCL and LCL abnormalities were defined as positive if their imaging appearance was classified as a Grade 1–3 collateral ligament tear, according to criteria defined previously.[22] Tendinosis was defined as positive in instances of elevated intramural signal or tendon thickening.

All readers first scored the DESS-only scan, and subsequently scored DESS combined with the conventional protocol (DESS+Conv). In a subset of 20 patients, three of the five readers scored the DESS scan first, then DESS with an additional coronal PDFS sequence (DESS +PDFS technique), and finally with DESS+Conv (overall study schematic in Fig. 1). Clinical information was not made available to the readers to ensure comparisons were made using imaging findings alone.

Comparison Metrics

The goal of this study was to compare the imaging appearance of knee abnormalities from the DESS and DESS+PDFS protocol to the conventional 2D imaging protocol. Consequently, the primary comparisons in findings were made in comparison to DESS +Conv, as that would provide the maximum amount of potential diagnostic information and

also because only a limited number of patients at our institution undergo interventional arthroscopies. Of all the patients scanned with the DESS sequence in this study, only nine underwent an additional arthroscopy, while only four patients from the DESS+PDFS cohort underwent surgery. As a result, comparisons with arthroscopy were only made in these limited cohorts for qualitative purposes. Arthroscopic surgery was used to determine the incidence of cartilage lesions, meniscal tears, synovitis, and tears of the anterior and posterior cruciate ligaments (ACL and PCL, respectively). Cartilage degeneration with arthroscopy was assessed using the Noyes criteria using Grades 1–4.[23]

Statistical Analysis

Since the primary diagnostic comparisons were being performed with reference to the DESS +Conv imaging findings, positive percentage agreement (PPA) and negative percentage agreement (NPA) and their 95% confidence intervals (CIs) for the DESS and DESS+PDFS techniques for each tissue type were used in lieu of sensitivity and specificity. PPA was determined when an abnormality was detected both in the reference standard (DESS+Conv) and the corresponding index test (either DESS or DESS+PDFS). Similarly, NPA was determined when an abnormality was not detected in the reference standard and either index test. Differences in the diagnostic accuracy measurements for the DESS and DESS+PDFS sequences were tested using exact McNemar tests. The percentage of observations where DESS or DESS+PDFS had equivalent confidence ratings to DESS+Conv were tested with exact symmetry tests. All diagnostic comparisons and confidence readings were pooled across patients and readers. Differences between readers in confidence ratings were tested by Cochran-Mantel-Haenszel tests stratified by patient.

Krippendorff's alpha (KA) coefficients were used to evaluate interobserver agreement.[24] Random-effects models accounting for multiple measurements within patients and readers were used to: 1) estimate the intraclass correlation (ICC) among readers for each outcome and method combination; 2) estimate the ICC between pairs of methods for each outcome; and 3) estimate the probability of a disagreement between pairs of methods, and test if they are different.

For the limited arthroscopic comparisons, sensitivity and specificity and their 95% CIs were calculated. Although the sample size of patients was limited and the prevalence of abnormalities was low, differences in the diagnostic accuracy measurements between DESS, DESS+PDFS, and DESS+Conv, compared with arthroscopy were tested using Cochran-Mantel-Haenszel tests stratified by protocol (accounting for unequal sample sizes per group). All statistical analyses were performed using Stata Release 14.2 (StataCorp, College Station, TX) with a significance level of 0.05.

Results

One patient was excluded due to excessive motion artifacts in the DESS scan. The conventional protocol required an average duration of 19 ± 3 minutes (two instances of repeated scans). The DESS scan by itself had a PPA of 90% (88–92% CI) and NPA of 99% (99–99% CI) in assessing the 30 abnormalities (Table 3). DESS had high PPA for diagnosing abnormalities of cartilage, menisci, tendons, and synovium; however, the PPA

was lower for ligament injuries. DESS+PDFS significantly increased PPA to 99% (95–99% CI) and the NPA to 100% (99–100% CI) compared with DESS alone (both $P < 0.001$).

DESS had equivalent diagnostic confidence to DESS+Conv in 94% of findings (Table 4), whereas DESS+PDFS had equivalent diagnostic confidence in 99% of findings (significantly higher than DESS alone, $P < 0.001$). There was a small, but significant, difference between reader agreement for diagnostic confidence scores for the DESS and DESS+PDFS techniques (both $P < 0.001$), but not the DESS+Conv sequences ($P = 0.16$). In comparison to arthroscopy, there were small, but statistically significant ($P < 0.01$), variations between the overall sensitivities (38%, 32%, and 41%, respectively, for DESS, DESS+PDFS, and the conventional protocol) and specificities (88%, 94%, 89%, respectively) between the three protocols (Table 5), indicating adequate interreader agreement across the protocols.

The observed agreement between readers (80–85%) for all three techniques was significantly higher than chance alone (~75%) ($P < 0.001$). KA values (47–48%) for all three techniques (Table 4) among all five of the readers indicated moderate interreader agreement. The ICC values for all readers for DESS, DESS+PDFS, and DESS+Conv were 0.78 (0.72–0.82), 0.77 (0.72–0.82), and 0.76 (0.71–0.81), respectively. ICC values between pairs of methods for each outcome were as follows: DESS+Conv vs. DESS: 0.74 (0.68–0.79); DESS +Conv vs. DESS+PDFS: 0.76 (0.70–0.81); DESS vs. DESS+PDFS: 0.85 (0.81–0.88). The probability of disagreement for the same pairs were 1.8% (1.4%–2.2%), 0.3% (0.2–0.5%), and 1.7% (1.3–2.1%), respectively, with a significant difference ($P < 0.001$) compared between DESS+Conv vs. DESS.

Derangement Examples

An arthroscopically confirmed full thickness ACL tear appeared similarly on both the DESS S− image and the T_2-weighted FS sequence, with disruption of fibers in the mid-portion of the ligament (Fig. 2a,b). While the T_2 relaxation times of healthy cartilage and a healthy ACL are ~30–35 msec and 10 msec, respectively, the corresponding T_2 values in the injured ACL were similar to those of the surrounding cartilage (Fig. 2c).[18,25] The high fluid-sensitivity of DESS was useful for diagnosing joint effusion, where the size and texture of joint effusion (dotted arrows Fig. 2a) was comparable to that of the T_2-weighted sequence (dotted arrows Fig. 2b), which helped in synovitis assessment. DESS, however, did underestimate the size of a bone marrow lesion (BML) adjacent to the ACL tear, compared with a conventional T_2-weighted scan (Fig. 2d–f).

An arthroscopically confirmed tear of the medial meniscus appeared similarly in the DESS S − image and the PD-weighted image, with increased signal in the posterior horn of the medial meniscus extending to the tibial articular surface (Fig. 3a,b). The corresponding DESS T_2 maps (Fig. 3c) also demonstrated higher T_2 values in the location of the tear. Similarly, the coronal reformation of the DESS image data and T_2 map (Fig. 3d,e), and the coronal PDFS sequence (Fig. 3f), showed high contrast for the tear. A region of Grade 3 cartilage degeneration in the femoral condyle was also well depicted by the DESS images and T_2 map.

The sagittal DESS images and the corresponding MPRs depicted examples of small arthroscopically confirmed cartilage lesions in the femoral trochlea (boxes Fig. 4a,b). The low-signal-intensity lesions appeared similarly on the DESS S− echo (Fig. 4a) and the T_2-weighted FS scan (Fig. 4b). The lesions were also highlighted using the focal and heterogeneous DESS T_2 relaxation values (Fig. 4c). Axial reformations of the lesion also indicated good conspicuity of the lesion in the DESS S + image and T_2 map, as compared with the conventional PD-weighted sequence (Fig. 4d–f). In an example of a patient with a signal arthroscopically confirmed abnormalities of the patellar and femoral cartilage, it could be seen that the abnormality was identified similarly on the second echo of DESS (Fig. 5a), the DESS T_2 map (Fig. 5d), and the T_2-weighted sequence (Fig. 5b). However, the signal variation was more challenging to identify on the first echo (S+) of DESS (Fig. 5c), which suggests that separating the two DESS echoes and creating T_2 maps may have higher diagnostic value than using a single combined image. Additionally, DESS was able to produce coronal oblique and axial reformations to better depict the region of low signal intensity in the patellar cartilage (Fig. 5e,f).

Discussion

In this study, a 5-minute 3D-DESS scan with separate echo images provided a similar imaging appearance for knee abnormalities as a conventional knee MRI protocol for diagnosing 30 internal knee abnormalities. The multicontrast DESS images with multiplanar reformations provided complementary diagnostic information sensitive to morphology and fluid signals. Many of the abnormalities were visualized well in the second (S−) echo, which had a higher T_2 weighting than the first (S+) echo. DESS did not require specialized reconstruction packages or hardware, making it clinically feasible. The abbreviated protocol consisting of an additional 2-minute PDFS sequence addressed the drawbacks of DESS, and produced high agreement with the conventional imaging protocol.

Chondral abnormalities were well visualized with DESS, which was expected since DESS has been used extensively for imaging cartilage and since the DESS sequence used in this study included fat-saturation, high-resolution, and high signal intensities.[19,26] Cartilage lesions were detected as regions of heterogeneous signal, whereas regions of fissuring and fibrillation were visualized due to the high resolution of the sequence. There have been previous studies reporting that chondral abnormalities are challenging to visualize with DESS, but these only included a single combined DESS echo.[27] The second echo of DESS has an increased T_2-weighting that lowers the sensitivity to susceptibility artifacts, which was useful in assessing cartilage fibrillation. In instances where the two DESS echo images are combined into a single composite image, the composite image contrast is dominated by the first echo (S+) image due its considerably higher SNR, compared with the second echo (S−) image. As a result, since composite images may have a lower influence on T_2-weighting and higher sensitivity to susceptibility artifacts, chondral lesions may be missed, as was demonstrated in this study. This may also explain the lower sensitivity of previous studies in detecting chondral lesions.[27] The impact of such an occurrence was mitigated in this study by simply separating the DESS echo images rather than combining them to form a composite image. This results in a higher overall T_2-weighting for the second echo of DESS.

Most subregions of the cartilage could be assessed in the sagittal plane; however, the axial reformations were useful for assessing the patellar and femoral trochlear cartilage. Most cartilage abnormalities had increased T_2 values and high signal intensity on the DESS S− echo, possibly indicative of fiber disorganization and water infiltration into the collagen.[28] However, some lesions had lower T_2 values, possibly due to collagenase-induced collagen cleavage leading to additional interacting sites between collagen and water.[28,29] Additionally, cartilage fibrillation has been thought to decrease the T_2 of adsorbed surface water and the adjacent mobile water protons through chemical exchange, resulting in regions of hypointense signal.[30] Combining routine T_2 measurements with morphological imaging may thus identify regions of cartilage damage, and potentially highlight regions with early degenerative changes.

The DESS echo images with varied contrasts were particularly useful in assessing abnormalities of the menisci, ligaments, and tendons—commonly injured tissues in the knee. The short echo time (TE) of the S + echo provided moderate SNR for visualizing the morphology of these tissues, while the lower SNR and fluid sensitivity of the S− echo was particularly useful in diagnosing meniscal and ligament tears. Healthy tissues had minimal S − signal, but tears caused fluid leakage into these tissues, which was well identified with the contrast, resolution, and T_2 measures provided by DESS. These results correspond with previous studies that demonstrate the benefit of T_2-weighted imaging for detecting lesions of the menisci and ligaments due to elevated signals in the lesion.[31] Even very subtle myxoid degeneration of the menisci and ligaments, which is usually indicated with an elevated signal, was well detected by DESS. The MPR capability generated additional perspectives to confirm the presence of such abnormalities in multiple scan orientations. Similar to menisci and ligaments, healthy tendons had moderate S + signal and minimal S− signal. However, the presence of any visible S− signal was more suggestive either of tendinosis or possibly a tendon rupture. The fluid sensitivity of the DESS S− echo also helped identify synovial abnormalities as well as cysts and cystic changes in the bone.

To date, there are few studies that have evaluated the utility of T_2 measurements in diagnostic clinical imaging, and such studies typically only assessed cartilage lesions.[28,32,33] While T_2 measurements in this study helped indicate cartilage lesions, they were also helpful in visualizing injuries to the menisci, ligaments, and tendons. The DESS S + TE (6 msec) was not short enough to accurately characterize the true T_2 values of healthy tendons and ligaments; however, it was adequate in assessing the substantially higher T_2 of injured tissues. If future studies require more accurate short-T_2 assessments, the ultrashort TE DESS sequence can produce TEs under 50 μs with isotropic resolution.[25] Overall, T_2 relaxation time mapping could provide complementary information to morphological imaging, aiding in the diagnosis of internal derangement, especially because no additional scan time or pulse sequences are required to generate this novel information.

In addition to evaluating the diagnostic utility of DESS with separated echoes, the second goal of this study was to evaluate the diagnostic potential of a fast high-resolution 3D sequence combined with one sequence from the conventional protocol. For this secondary goal, DESS was paired with the coronal PDFS sequence. One drawback of DESS was MPR-induced blurring due to the anisotropic voxel acquisition, which obscured the visualization

of the thin collateral ligaments. An additional drawback was that DESS underestimated the size of bone marrow lesions (BMLs) due to trabecular T_2^* susceptibility effects and complicated relationships of the T_2/T_1 ratios of the lesions, which affect the steady-state signal.[19,34] With these drawbacks in mind, the FSE coronal PDFS sequence was ideal for assessing the collateral ligaments and BMLs. A combination of the high-resolution of sagittal DESS and coronal PDFS thereby enabled accurate assessment of all abnormalities evaluated in this study. Future studies could lower the in-plane resolution of DESS to match that of the 2D FSE sequences (~0.5 × 0.5 mm) to enable scanning 2× thinner slices without a loss in SNR based on voxel volume. Additional methods could also include DESS with 3D radial sampling for acquiring images with isotropic resolutions or use deep learning to enhance through-plane resolution without biasing quantitative T_2 accuracy.[25,35,36] The current study also utilized an 8-channel transmit/receive coil for imaging due to its pervasive use in knee imaging; however, higher element knee coils exist, which could be used to further enhance scans based on improved coil-sensitivity and g-factor conditioning.

The arthroscopic correlations in the small subset of patients showed relatively comparable accuracy with previous studies, albeit with slightly lower sensitivities.[37,38] This was promising, because the goal of this study was not to compare the DESS and DESS+PDFS findings with arthroscopy. Consequently, the readers were not provided with patient history, reason for referral, and previous imaging and surgical findings. The specificities of diagnosing injuries of the meniscus, ligaments, and tendons were high, whereas the sensitivities of diagnosing such lesions were lower (especially in cartilage), which has been chronicled in previous studies.[37,38] Of the two ACL tears observed in the nine patients, one was correctly identified by all readers, while a subtle tear was missed by all readers, leading to the lower 50% sensitivity. The overall results of the arthroscopic comparisons remained consistent among all three protocols, demonstrating that there was likely no consistent bias induced by any single protocol.

Regarding study design, DESS+Conv was chosen as the reference standard over arthroscopy, as diagnostic arthroscopies are not performed in all patients, especially after unremarkable MRIs. Additionally, even with arthroscopy, it is challenging to evaluate all the abnormalities analyzed in this study and there can exist considerable interreader variability for assessing chondral lesions.[39] Interpreting all scans starting with the DESS sequence would produce the most conservative accuracy estimates and reduce the false-finding rates, in case DESS provided diagnostic information not contained in the conventional protocol. Moreover, using DESS+Conv as the reference standard would provide radiologists with the maximum imaging information possible and allow for head-to-head sequence comparisons, justifying its usage as the reference standard for evaluating agreement for the rapid sequences.

Compared with similar previous studies, this study had a larger number of abnormalities being assessed in order to evaluate true utility for whole-joint diagnostic imaging.[6,8,9] It also had considerably more readers in order to ensure sequence robustness by collating responses from multiple readers with varying experience levels, expertise, and methodologies for making clinical diagnoses. Three readers were trained in the US (C.B., G.G., and J.W.), while two were trained in Europe (K.S. and E.O.). At the time of the study, one practices in

Europe (E.O.) and one was a clinical fellow (J.W.), which depicts the heterogeneity of the readers involved. Despite this breadth of experience, there existed consistency among the readers and among the sequences, as indicated by the high ICC values and low probabilities for disagreement between protocols.

This study also had certain limitations. The readers for this study could not be blinded to the sequences being used due to the inherent image contrasts. Despite the promising preliminary results presented here, additional subjects will be required in future studies for more robust statistical outcomes. Having arthroscopic comparisons in all patients will also provide an additional metric for the accuracy of the DESS scans. While analyzing all three protocols in succession may produce the most diagnostic information for the reference standard, it may also introduce a memory-related reader bias. Future studies could include washout durations between protocols in order to minimize memory bias. The study protocol utilized in this article did not contain a nonfat-saturated sequence, which may limit the sensitivity to osseous abnormalities. Consequently, subsequent work could explore implementing a Dixon-based proton-density-weighted sequence to generate fat, water, in-phase, and out-of-phase image contrasts.[40] Future work could also explore mitigating the MPR-induced blurring by evaluating the tradeoffs between in-plane and slice resolution. Additionally, the T_2 relaxation time maps were retrospectively correlated with the abnormalities described by the reader. However, given the potential benefits of incorporating T_2 measurements into routine diagnostic imaging, future studies could be performed for prospectively using the T_2 measurements. Furthermore, optimization of the protocols of pulse sequences used in this study for 1.5T scanners may also be beneficial, given the widespread use of 1.5T for extremity MRI.

In conclusion, we have demonstrated that 1) a single 5-minute 3D-DESS sequence with separated echoes depicted knee abnormalities similarly to a clinical knee MRI protocol, and 2) a 5-minute DESS sequence with separated echoes paired with a 2-minute coronal PDFS sequence may be one potential path towards an abbreviated knee MRI protocol. Consequently, the results from this study support further evaluation of the utility of the two techniques in larger studies, especially with the incorporation of T_2 relaxation time measurements.

Acknowledgments

Contract grant sponsor: National Institutes of Health (NIH); Contract grant numbers: NIH R01 AR063643, R01 EB002524, K24 AR062068, and P41 EB015891; Contract grant sponsor: GE Healthcare (research support).

References

1. Hing E, Rui P, Palso K. National Ambulatory Medical Care Survey: 2013 State and National Summary Tables. 2013;1:Table 21.
2. Rinck P What is the Organ Distribution of MRI Studies? Eur Magn Reson Forum – EMRF 2005.
3. van Beek EJR, Kuhl C, Anzai Y, et al. Value of MRI in medicine: More than just another test? J Magn Reson Imaging 2018;47:1–12.
4. Alaia EF, Benedick A, Obuchowski NA, et al. Comparison of a fast 5-min knee MRI protocol with a standard knee MRI protocol?: A multi-institutional multi-reader study. Skeletal Radiol 2018;47:107–116. [PubMed: 28952012]

5. Fritz J, Fritz B, Zhang J, et al. Simultaneous multislice accelerated turbo spin echo magnetic resonance imaging: Comparison and combination with in-plane parallel imaging acceleration for high-resolution magnetic resonance imaging of the knee. Invest Radiol 2017;52:529–537. [PubMed: 28430716]
6. Fritz J, Ahlawat S, Fritz B, et al. 10-Min 3D turbo spin echo MRI of the knee in children: Arthroscopy-validated accuracy for the diagnosis of internal derangement. J Magn Reson Imaging 2018;47:1–13.
7. Bao S, Tamir JI, Young JL, et al. Fast comprehensive single-sequence four-dimensional pediatric knee MRI with T2 shuffling. J Magn Reson Imaging 2016;45:1–12.
8. Kijowski R, Davis KW, Woods MA, et al. Knee joint: Comprehensive assessment with 3D isotropic resolution fast spin-echo MR imaging—Diagnostic performance compared with that of conventional MR imaging at 3.0 T. Radiology 2009;252:486–495. [PubMed: 19703886]
9. Duc SR, Pfirrmann CWA, Koch PP, Zanetti M, Hodler J. Internal knee derangement assessed with 3-minute three-dimensional isovoxel true FISP MR sequence: Preliminary study. Radiology 2008;246:526–535. [PubMed: 18227545]
10. Kijowski R, Blankenbaker DG, Klaers JL, Shinki K, De Smet AA, Block WF. Vastly undersampled isotropic projection steady-state free precession imaging of the knee: Diagnostic performance compared with conventional MR. Radiology 2009;251:185–194. [PubMed: 19221057]
11. Bruder H, Fischer H, Graumann R, Deimling M. A new steady-state imaging sequence for simultaneous acquisition of two MR images with clearly different contrasts. Magn Reson Med 1988;7:35–42. [PubMed: 3386520]
12. Redpath TW, Jones RA. FADE—a new fast imaging sequence. Magn Reson Med 1988;6:224–234. [PubMed: 3367779]
13. Lee SY, Cho ZH. Fast SSFP gradient echo sequence for simultaneous acquisitions of FID and echo signals. Magn Reson Med 1988;8:142–150. [PubMed: 3210952]
14. Chaudhari AS, Black MS, Eijgenraam S, et al. Five-minute knee MRI for simultaneous morphometry and T 2 relaxometry of cartilage and meniscus and for semiquantitative radiological assessment using double-echo in steady-state at 3T. J Magn Reson Imaging 2018;47:1328–1341. [PubMed: 29090500]
15. Hunter DJ, Guermazi A, Lo GH, et al. Evolution of semi-quantitative whole joint assessment of knee OA: MOAKS (MRI Osteoarthritis Knee Score). Osteoarthr Cartil 2011;19:990–1002.
16. Welsch GH, Mamisch TC, Domayer SE, et al. Cartilage T2 assessment at 3-T MR imaging: in vivo differentiation of normal hyaline cartilage from reparative tissue after two cartilage repair procedures—Initial experience. Radiology 2008;247:154–161. [PubMed: 18372466]
17. Staroswiecki E, Granlund KL, Alley MT, Gold GE, Hargreaves BA. Simultaneous estimation of T2 and apparent diffusion coefficient in human articular cartilage in vivo with a modified three-dimensional double echo steady state (DESS) sequence at 3 T. Magn Reson Med 2012;67: 1086–1096. [PubMed: 22179942]
18. Dunn TC, Lu Y, Jin H, Ries MD, Majumdar S. T2 relaxation time of cartilage at MR imaging: Comparison with severity of knee osteoarthritis. Radiology 2004;232:592–598. [PubMed: 15215540]
19. Peterfy CG, Schneider E, Nevitt M. The osteoarthritis initiative: Report on the design rationale for the magnetic resonance imaging protocol for the knee. Osteoarthr Cartil 2008;16:1433–1441.
20. Blaimer M, Breuer F, Mueller M, Heidemann RM, Griswold MA, Jakob PM. SMASH, SENSE, PILS, GRAPPA: How to choose the optimal method. Top Magn Reson Imaging 2004;15:223–236. [PubMed: 15548953]
21. Sveinsson B, Chaudhari A, Gold G, Hargreaves B. A simple analytic method for estimating T2 in the knee from DESS. Magn Reson Imaging 2017;38:63–70. [PubMed: 28017730]
22. Schweitzer ME, Tran D, Deely DM, Hume EL. Medial collateral ligament injuries: Evaluation of multiple signs, prevalence and location of associated bone bruises, and assessment with MR imaging. Radiology 1995; 194:825–829. [PubMed: 7862987]
23. Noyes FR, Stabler CL. A system for grading articular cartilage lesions at arthroscopy. Am J Sports Med 1989;17:505–513. [PubMed: 2675649]

24. Krippendorf K Reliability in content analysis: Some common misconceptions and recommendations. Hum Commun Res 2004;30:411–433.
25. Chaudhari AS, Sveinsson B, Moran CJ, et al. Imaging and T2 relaxometry of short-T2 connective tissues in the knee using ultrashort echo-time double-echo steady-state (UTEDESS). Magn Reson Med 2017;78: 2136–2148. [PubMed: 28074498]
26. Kohl S, Meier S, Ahmad SS, et al. Accuracy of cartilage-specific 3-Tesla 3D-DESS magnetic resonance imaging in the diagnosis of chondral lesions: Comparison with knee arthroscopy. J Orthop Surg Res 2015; 10:191. [PubMed: 26714464]
27. Roemer FW, Kwoh CK, Hannon MJ, et al. Semiquantitative assessment of focal cartilage damage at 3 T MRI: A comparative study of dual echo at steady state (DESS) and intermediate-weighted (IW) fat suppressed fast spin echo sequences. Eur J Radiol 2011;80:126–131.
28. Kijowski R, Blankenbaker DG, Munoz Del Rio A, Baer GS, Graf BK. Evaluation of the articular cartilage of the knee joint: Value of adding a T2 mapping sequence to a routine MR imaging protocol. Radiology 2013; 267:503–513. [PubMed: 23297335]
29. Hodler J, Berthiaume MJ, Schweitzer ME, Resnick D. Knee joint hyaline cartilage defects: A comparative study of MR and anatomic sections. J Comput Assist Tomogr 1992;16:597–603. [PubMed: 1629420]
30. Mosher TJ, Pruett SW. Magnetic resonance imaging of superficial cartilage lesions: Role of contrast in lesion detection. J Magn Reson Imaging 1999;10:178–182. [PubMed: 10441022]
31. Mink JH, Levy T, Crues JV. Tears of the anterior cruciate ligament and menisci of the knee: MR imaging evaluation. Radiology 1988;167: 769–774. [PubMed: 3363138]
32. Hannila I, Nieminen MT, Rauvala E, Tervonen O, Ojala R. Patellar cartilage lesions: Comparison of magnetic resonance imaging and T2 relaxation-time mapping. Acta Radiol 2007;48:444–448. [PubMed: 17453527]
33. Apprich S, Welsch GH, Mamisch TC, et al. Detection of degenerative cartilage disease: Comparison of high-resolution morphological MR and quantitative T2 mapping at 3.0 Tesla. Osteoarthr Cartil 2010;18: 1211–1217.
34. Yoshioka H, Stevens K, Hargreaves BA, et al. Magnetic resonance imaging of articular cartilage of the knee: Comparison between fat-suppressed three-dimensional SPGR imaging, fat-suppressed FSE imaging, and fat-suppressed three-dimensional DEFT imaging, and correlation with arthroscopy. J Magn Reson Imaging 2004;20:857–864. [PubMed: 15503323]
35. Chaudhari AS, Fang Z, Kogan F, et al. Super-resolution musculoskeletal MRI using deep learning. Magn Reson Med 2018;80:2139–2154. [PubMed: 29582464]
36. Chaudhari A, Fang Z, Lee JH, Gold G, Hargreaves B. Deep learning super-resolution enables rapid simultaneous morphological and quantitative magnetic resonance imaging. In: Int Work Mach Learn Med Image Reconstr 2018:3–11.
37. Nikolaou VS, Chronopoulos E, Savvidou C, et al. MRI efficacy in diagnosing internal lesions of the knee: A retrospective analysis. J Trauma Manag Outcomes 2008;2:4. [PubMed: 18518957]
38. Reed ME, Villacis DC, Hatch GFR, et al. 3.0-Tesla MRI and arthroscopy for assessment of knee articular cartilage lesions. Orthopedics 2013;36: e1060–1064. [PubMed: 23937754]
39. Spahn G, Klinger HM, Hofmann GO. How valid is the arthroscopic diagnosis of cartilage lesions? Results of an opinion survey among highly experienced arthroscopic surgeons. Arch Orthop Trauma Surg 2009;129: 1117–1121. [PubMed: 19367409]
40. Kogan F, Chaudhari AS, Black MS, et al. High patient throughput 5-minute comprehensive quantitative bilateral knee MRI. Proc Intl Work Osteo Imaging 2018 [Epub ahead of print].

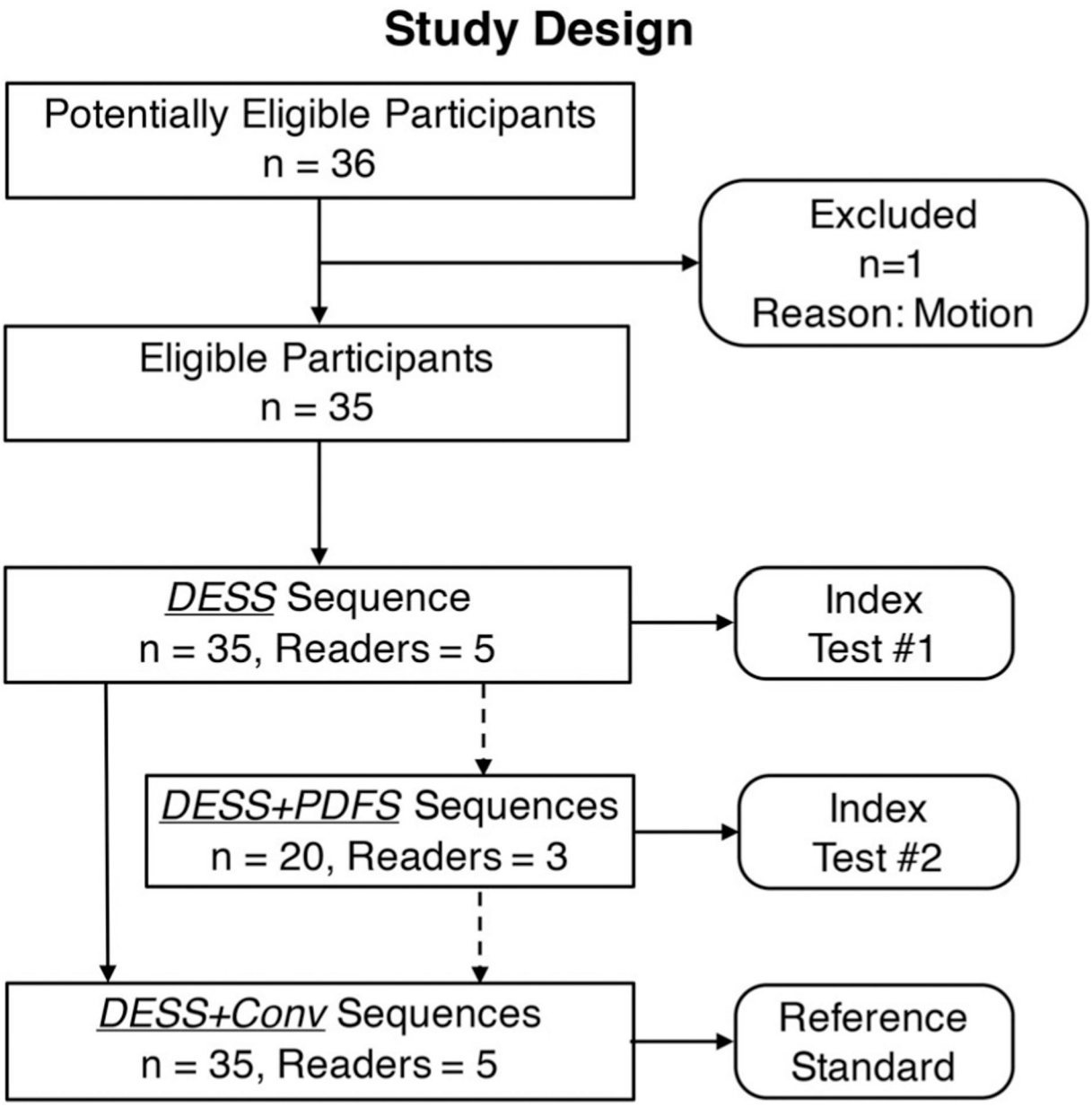

FIGURE 1:
Schematic for the proposed study utilizing the double-echo in steady-state (DESS) pulse sequence with separated echoes with and without pairing a coronal proton-density-weighted fat-saturated (PDFS) sequence. Imaging findings from DESS combined with the conventional imaging protocol (DESS+Conv) were used as the comparison standard.

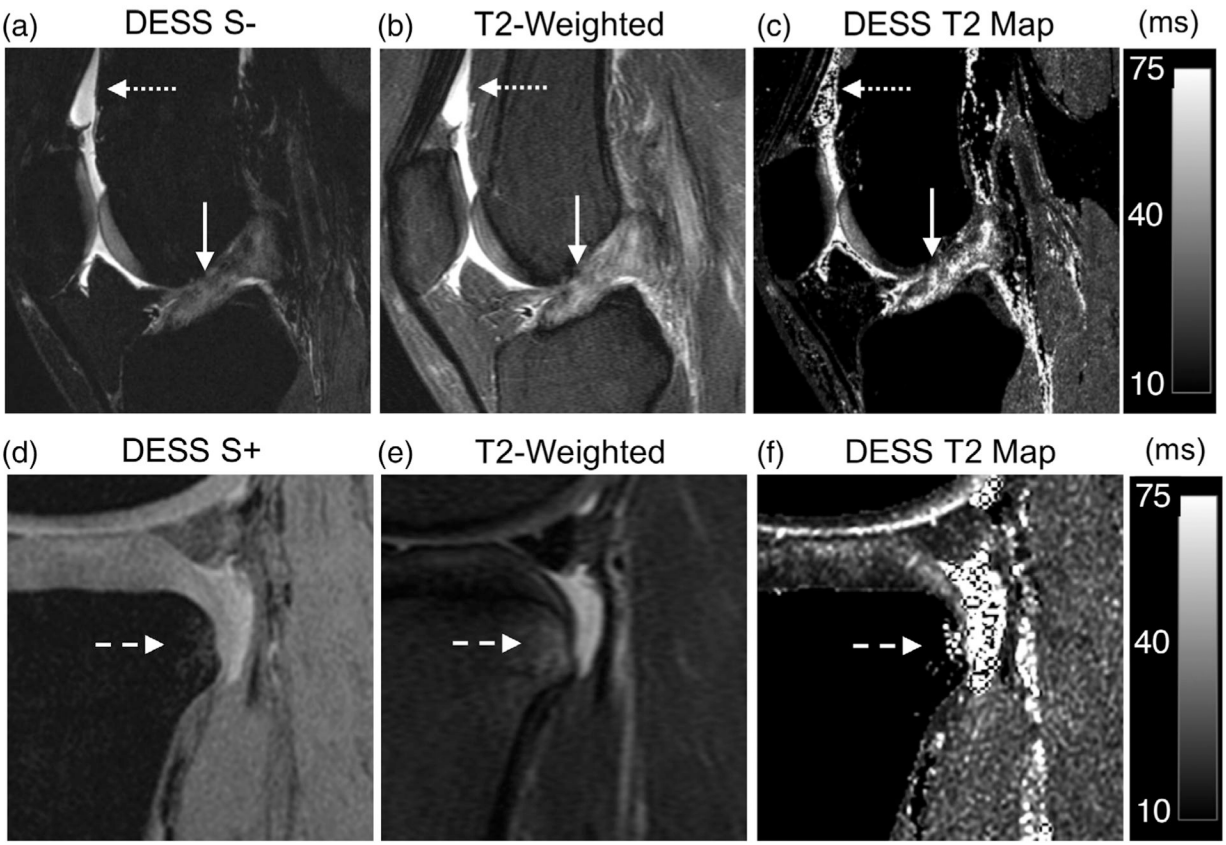

FIGURE 2:

A 19-year-old female presenting discontinuity of the anterior cruciate ligament (ACL) fibers, compatible with a complete tear (solid arrow) and mild joint effusion (dotted arrow). **(a)** A sagittal water-excitation DESS S− image demonstrates increased signal in the ACL and discontinuity of the ligament fibers as well high fluid contrast for the joint effusion. **(b)** A sagittal T_2-weighted fat-saturated scan similarly demonstrates a full thickness tear of the ACL and increased signal intensity for the synovial fluid. **(c)** An instantly generated DESS T_2 relaxation time map shows elevated T_2 values of the ACL (similar to that of adjacent cartilage) and focal regions of fluid signals. **(d)** A bone marrow lesion (BML) in the same patient (dotted arrows) in the posterior tibial condyle is underestimated in volume by the DESS S + image. **(e)** A T_2-weighted scan depicts the actual size of the BML. **(f)** The DESS T_2 map shows the T_2 of the BML with the same volume as the S + image.

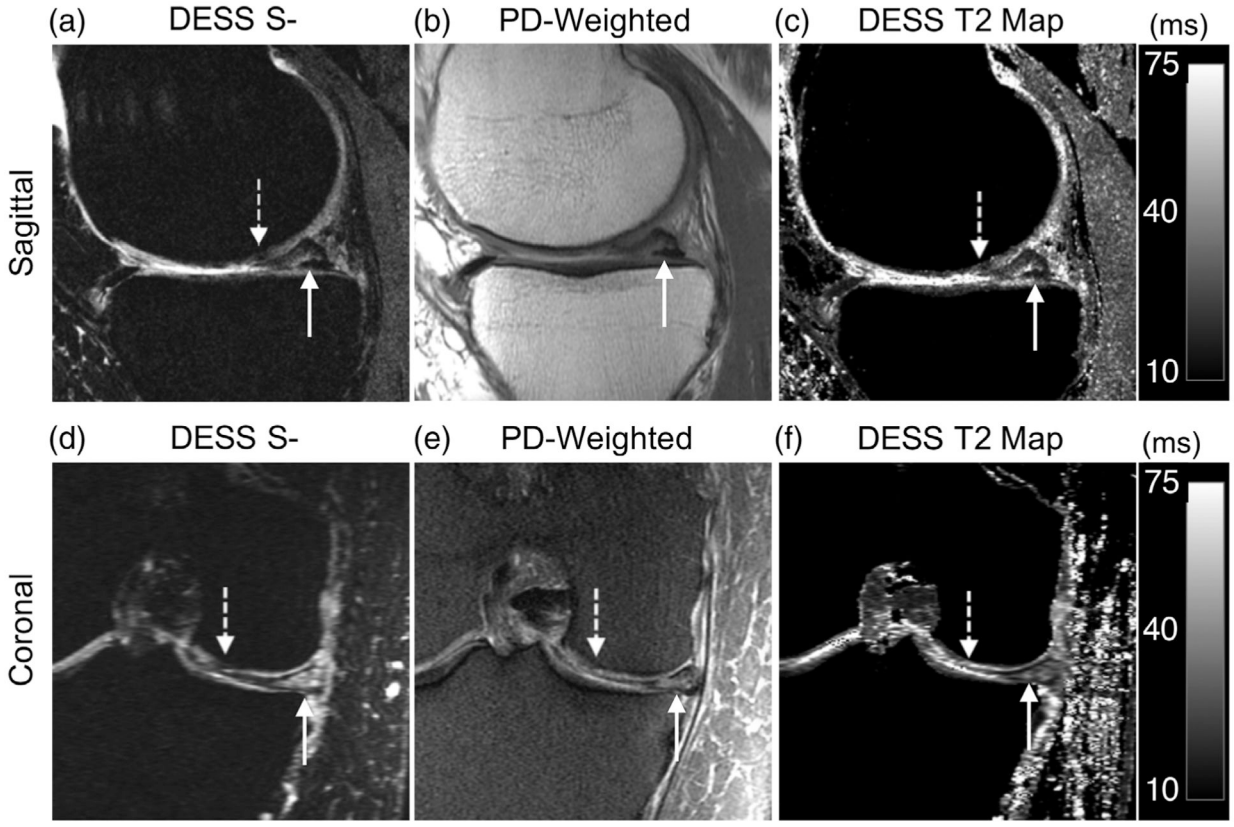

FIGURE 3:

A 74-year-old male presenting with an arthroscopically confirmed tear of the posterior horn of the medial meniscus and Grade 3 cartilage degeneration in the femoral condyle. **(a)** A sagittal water-excitation DESS S− image demonstrates increased signal in the meniscus extending to the tibial articular surface (solid arrow) and a focal region of cartilage damage in the femoral condyle (dotted arrow). **(b)** A sagittal proton-density-weighted scan from the conventional protocol demonstrates the meniscal tear. **(c)** A DESS T_2 relaxation time map shows elevated T_2 values of the meniscus tear and a region of hypointense cartilage T_2 values in the femoral condyle. **(d)** A coronal reformation of the water-excitation DESS S− also demonstrates increased signal in the meniscus, compatible with a meniscal tear and a region of cartilage signal heterogeneity in the femoral condyle. **(e)** A coronal proton-density-weighted fat-saturated scan depicts similar contrast for the meniscal tear. **(f)** A quantitative coronal DESS T_2 map reformation highlights the meniscal tear and cartilage degeneration abnormalities.

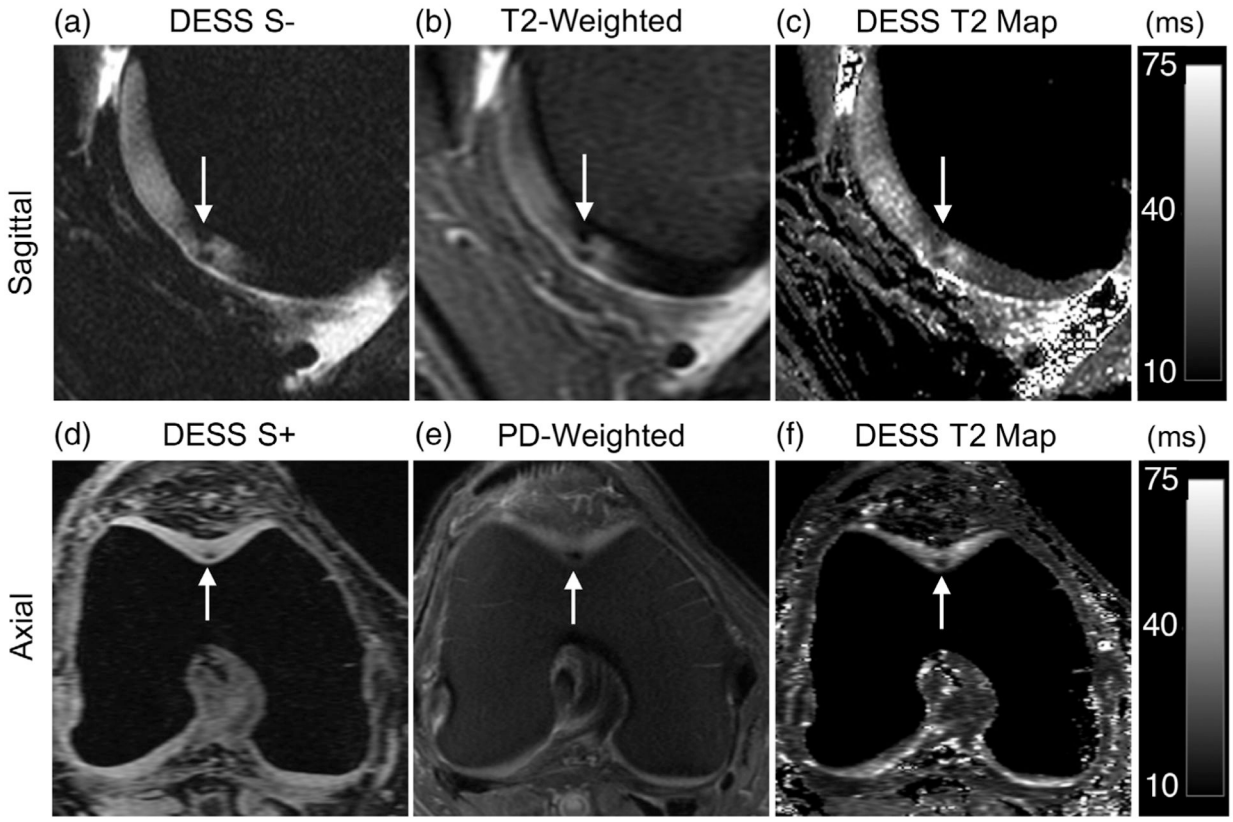

FIGURE 4:

A 65-year-old female presenting chondral lesions in the femoral trochlea (solid arrow). **(a)** A sagittal water-excitation DESS S− image shows focal hypointense regions in the femoral trochlear cartilage. **(b)** A sagittal T_2-weighted fat-saturated scan similarly demonstrates the hypointense regions of cartilage with similar size and intensity. **(c)** An instantly generated DESS T_2 relaxation time map shows lowered T_2 of the chondral lesion compared with that of the surrounding cartilage. **(d)** Axial reformations of the DESS sequence help characterize the size and location of the lesions. **(e)** A proton-density (PD)-weighted image depicts the lesion with similar conspicuity as the DESS image. **(f)** The DESS T_2 map also highlights the location of the lesion with high contrast.

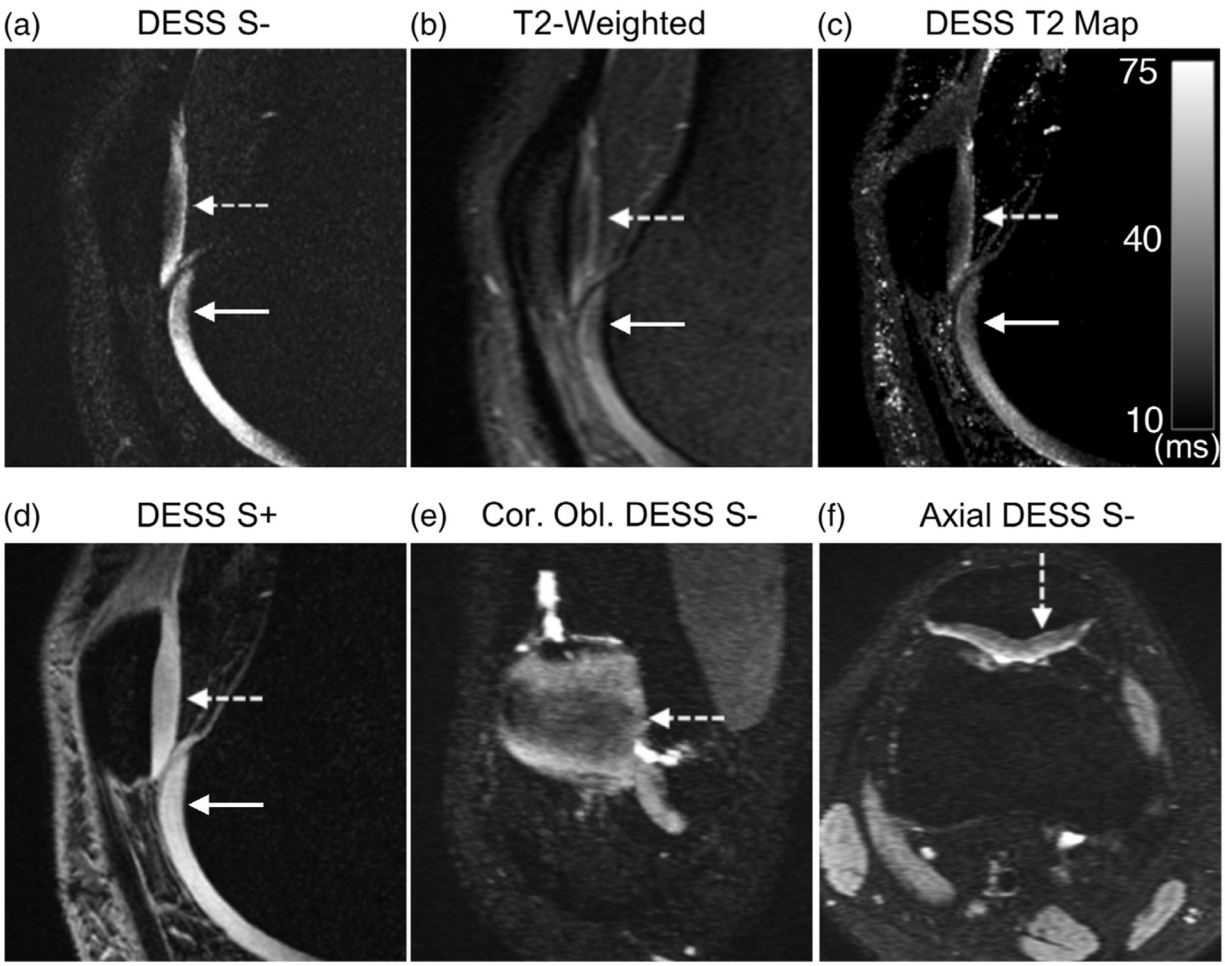

FIGURE 5:

A 26-year-old male presenting with a patellar cartilage (dotted arrow) and femoral cartilage (solid arrow) signal abnormality with two regions of hypointense signal. **(a)** A sagittal water-excitation DESS S− image shows the hypointense signal in the two cartilage regions. **(b)** A sagittal T_2-weighted fat-saturated scan also shows the hypointense signals in the region of the patellar and femoral trochlear cartilage. **(c)** A sagittal DESS S + image shows hypointense signals, but not as clearly as the DESS S− image. **(d)** The quantitative DESS T_2 map exhibits regions of lower T_2 values in the regions corresponding to the signal heterogeneity in the T_2-weighted and DESS S− image. **(e)** The DESS S− image can be used to create coronal oblique reformations to better view the patellar cartilage surface. **(f)** An axial reformation of the DESS S− image also depicts regions of hypointense cartilage signal for allowing a three-planar analysis of the signal abnormality.

TABLE 1.

Scan Parameters for All MRI Sequences Utilized in This Study

Protocol	**Conventional**					**DESS-Only**
Sequence	**2D Ax PD FS**	**2D Cor T1**	**2D Sag T2 FS**	**2D Sag PD**	**2D Cor PD FS**	**3D Sag DESS FS**
TR (msec)	4000	600	5441	4000	4000	18.6
TE S + (msec)	35	18	54	35	35	5.9
TE S- (msec)	N/A	N/A	N/A	N/A	N/A	31.3
Flip angle (°)	142	142	142	142	142	20
Echo train length	9	3	11	9	9	1
NEX	3	3	4	2	2	1
Bandwidth (± kHz)	50	50	50	50	50	41.7
FOV (cm)	14	14	14	14	14	16
Matrix (RO × PE)	512 × 224	416 × 224	384 × 192	384 × 224	384 × 224	416 × 512
Resolution (mm^2)	0.27 × 0.63	0.34 × 0.63	0.36 × 0.72	0.36 × 0.63	0.36 × 0.63	0.34 × 0.27
Slice thickness (mm)	3	2.5	2.5	2.5	2.5	1.6 (0.8)[a]
Slice spacing (mm)	0.3	0	0	0	0	0
Number of slices	36	44	40	40	44	80 (160)[a]
Parallel imaging	2 × 1	NA	2 × 1	NA	2 × 1	2 × 1
Scan time	2:56	2:18	3:43	3:28	2:00	5:00

[a]Note that slices were acquired at 1.6 mm slice thickness interpolated to 0.8 mm thicknesses. During review, slices in all orientations were viewed with 2.4 mm slice thickness. DESS utilized a slice direction spoiler gradient area of 31 $mT^1m^{-1}ms^1$ (1.33 cycles of dephasing/mm). Ax, axial; Cor, coronal; Sag, sagittal; PD, proton density; FS, fat saturated; DESS, double echo in steady state; TR, repetition time; TE, echo time; NEX, number of averages; FOV, field of view; RO, readout; PE, phase encodes.

TABLE 2.

All Readers Assessed the Presence or Absence of the Listed Abnormalities and Scored the Diagnostic Confidence of the Protocol From a Scale of 0 to 3 (0 = Lowest, 3 = Highest) for Each Abnormality

Tissue	Derangement	Tissue	Derangement
Bone	Bone marrow edema	Cartilage	Patellar defects[a]
	Fracture		Trochlear defects[a]
	Subchondral cyst		Medial femoral condyle defects[a]
	Fibro-osseous junction cystic change		Lateral femoral condyle defects[a]
Ligaments	ACL - Mucoid degeneration		Medial tibial plateau defects[a]
	ACL - Partial tear[a]		Lateral tibial plateau defects[a]
	ACL - Complete tear[a]	Meniscus	LM - Myxoid degeneration
	PCL - Mucoid degeneration		LM - Tear[a]
	PCL - Partial tear[a]		LM - Displaced fragment/flaps
	PCL - Complete tear[a]		MM - Myxoid degeneration
	MCL Abnormality		MM - Tear[a]
	LCL Abnormality		MM - Displaced fragment/flaps
	Posterolateral corner injury	Tendons	Pat/Quads Tendon - Tendinosis
Synovium	Joint effusion		Pat/Quads Tendon - Partial Tear
	Synovitis[a]		Pat/Quads Tendon - Complete Tear

[a]Indicates abnormalities assessed during arthroscopic surgery. LM, lateral meniscus; MM, medial meniscus; ACL, anterior cruciate ligament; PCL, posterior cruciate ligament; MCL, medial collateral ligament; LCL, lateral collateral ligament; Pat/Quads Tendon, patellar or quadriceps tendon.

TABLE 3.

Positive Percent Agreement (PPA) and Negative Percent Agreement (NPA) and the Corresponding Confidence Intervals (in Parentheses) Are Provided Along With the Positive and Negative Occurrence Counts for the DESS and DESS+PDFS Methods

	Bone	Cartilage	Meniscus	Ligaments	Tendons	Synovium	Overall
DESS Sequence							
PPA Occurrences	85 (78–91) 103/121	94 (89–97) 176/188	89 (82–93) 115/130	76 (63–86) 45/59	91 (71–99) 20/22	100(99–100) 112/112	90(89–92) 571/632
NPA Occurrences	99 (98–99) 573/579	99 (99–99) 858/862	99 (99–99) 914/920	99 (99–99) 1507/1516	99 (98–99) 499/503	99 (99–99) 235/238	99 (99–99) 4586/4618
DESS+PDFS Sequences							
PPA Occurrences	100(88–100) 28/28	100(91–100) 39/39	90(68–99) 18/20	100 (80–100) 17/17	100(59–100) 7/7	100(90–100) 36/36	9(95–99)* 145/147
NPA Occurrences	100(98–100) 212/212	100(99–100) 321/321	99(98–100) 338/340	100(99–100)** 523/523	100 (98–100) 173/173	100(97–100) 84/84	100(98–100)* 1651/1653

Significantly different comparisons between the DESS and DESS+PDFS methods are represented with * $P < 0.001$ and ** $P = 0.03$. All occurrence numbers indicated are pooled across all readers and patients.

TABLE 4.

Equivalent Diagnostic Confidence Percentage for DESS and DESS+PDFS Techniques and Interreader Agreement With Krippendorff's Alpha

	Bone	Cartilage	Meniscus	Ligaments	Tendons	Synovium	Overall
Equivalent Diagnostic Confidence %							
DESS Counts	94 (92–96) 661/700	96 (95–97) 1008/1050	97 (96–98) 1019/1050	89 (87–90) 1402/1575	98 (96–99) 514/525	99 (98–100) 347/350	94 (94–95) 4951/5250
DESS+PDFS Counts	100 (98–100) 240/240	100 (99–100) 360/360	99 (97–99) 355/360	99 (97–99) 532/540	98 (95–99) 177/180	100 (97–100) 120/120	99 (99–99) 1784/1800
Krippendorff's alpha (KA %)							
DESS	43	43	38	31	15	76	47
DESS+PDFS	45	42	35	38	8	75	48
DESS+Conv	43	42	38	34	8	70	47

All numbers for diagnostic confidence are pooled across all readers and patients.

TABLE 5.

Agreement Between Surgical Arthroscopy and the DESS and Conventional Protocol (Nine Patients Each), and the DESS+PDFS Technique (Four Patients)

	Sensitivity			Specificity		
Tissue	**DESS**	**DESS+PDFS**	**Conventional**	**DESS**	**DESS+PDFS**	**Conventional**
Meniscus	53 (36–69) 21/40	100 10/10	60 (43–75) 24/40	90 (78–97) 45/50	93 (78–99) 28/30	90 (78–97) 45/50
Ligaments	50 (19–81) 5/10	N/A 0/0	50 (19–81) 5/10	91 (77–98) 32/35	95 (75–99) 19/20	97 (85–99) 34/35
Synovitis	50 (29–71) 12/24	33 (8–70) 3/9	50 (29–71) 12/24	57 (34–78) 12/21	82 (48–98) 9/11	52 (30–74) 11/21
Cartilage Grade 1	12 (6–23) 8/65	12 (5–25) 7/55	12 (6–23) 8/65	—	—	—
Cartilage Grade 2	40 (21–61) 10/25	47 (21–73) 7/15	40 (21–61) 10/25	—	—	—
Cartilage Grade 3	41 (30–53) 31/75	40 (21–61) 10/25	48 (36–60) 36/75	—	—	—
Cartilage Grade 4	67 (38–88) 10/15	40 (5–86) 2/5	67 (38–88) 10/15	—	—	—
Cartilage Overall:	33 (26–40) 59/180	26 (18–36) 26/100	36 (29–43) 64/180	93 (86–98) 84/90	100 20/20	93 (86–98) 84/90
Total	38 (32–45) 97/254	32 (24–42) 39/119	41 (35–48) 105/254	88 (83–92) 173/196	94 (86–98) 76/81	89 (32–93) 174/196

Sensitivity, specificity, the corresponding confidence intervals (in parentheses) are provided along with the positive and negative occurrence counts of the DESS and DESS+PDFS methods. All occurrence numbers indicated are pooled across all readers and patients.